

Solid-state spun fibers and yarns from 1-mm long carbon nanotube forests synthesized by water-assisted chemical vapor deposition

Shanju Zhang · Lingbo Zhu · Marilyn L. Minus · Han Gi Chae ·
Sudhakar Jagannathan · Ching-Ping Wong · Janusz Kowalik ·
Luke B. Roberson · Satish Kumar

Received: 15 November 2007 / Accepted: 13 February 2008 / Published online: 18 April 2008
© Springer Science+Business Media, LLC 2008

Abstract We report continuous carbon nanotube (CNT) fibers and yarns dry-drawn directly from water-assisted chemical vapor deposition (CVD) grown forests with about 1-mm height. As-drawn CNT fibers exist as aerogel and can be transformed into more compact fibers through twisting or densification with a volatile organic liquid. CNT fibers are characterized by scanning electron microscopy, X-ray photoelectron spectroscopy, Raman microscopy, and wide-angle X-ray diffraction. Mechanical properties and electrical conductivity of the post-treated CNT fibers are investigated. The resulting fibers show the work of rupture of 30 J/g and DC electrical conductivity of 5.0×10^4 S/m.

Introduction

Carbon nanotubes (CNTs) are very promising candidates for the development of the next generation of high performance, lightweight fibers, and textiles with high modulus and strength. Breakthroughs have been made in coagulation spinning of single-wall (SWNTs) and multi-wall (MWNTs) nanotubes from polymer solution [1–3], in gas-state spinning of SWNTs and MWNTs from reaction furnace [4–6], in liquid crystalline wet spinning of SWNTs from super acids [7–9] as well as in solid-state spinning of MWNTs from vertically aligned nanotube forests [10–13]. Water-assisted chemical vapor deposition (CVD) synthesis represents a novel and promising process for size-selective growth of highly pure, very long, and vertically aligned CNT forests [14–18]. Millimeter long SWNTs [14, 15], MWNTs [16, 17], and double-wall nanotubes (DWNTs) [18] have been reported by adding a small amount of water into the CVD chamber. Longer nanotubes are expected to provide efficient mechanical load transfer, as well as electron and phonon transport [19]. In this work, we report continuous MWNT fibers and yarns dry-drawn from 1-mm high water-assisted CVD grown nanotube forests. The as-drawn fibers are twisted and subsequently densified to lock-in the effects from twisting. The mechanical and electrical properties of the post-treated fibers are investigated.

S. Zhang · M. L. Minus · H. G. Chae · S. Jagannathan ·
S. Kumar (✉)
School of Polymer, Textile and Fiber Engineering, Georgia
Institute of Technology, 801 Ferst Drive, Atlanta, GA 30332,
USA
e-mail: satish.kumar@ptfe.gatech.edu

S. Zhang
e-mail: szhang30@mail.gatech.edu

L. Zhu · C.-P. Wong
School of Materials Sciences and Engineering, Georgia Institute
of Technology, 771 Ferst Drive, Atlanta, GA 30332, USA

J. Kowalik
School of Chemistry and Biochemistry, Georgia Institute
of Technology, Atlanta, GA 30332, USA

L. B. Roberson
National Aeronautics and Space Administration,
John F. Kennedy Space Center, Kennedy Space Center,
Orlando, FL 32899, USA

Experimental part

Water-assisted CVD synthesis was performed in a horizontal alumina tube (3.8-cm diameter; 92-cm long) housed in a Lindberg Blue furnace [16, 17]. The substrates used in this study were (001) silicon wafers coated with 500-nm

thick layer of thermally grown SiO₂. The catalyst layers of Al₂O₃ (15 nm)/Fe (2 nm) were formed on the silicon wafer by sequential e-beam evaporation. CVD growth of CNTs was carried out at 750 °C with ethylene (150 sccm) as the carbon source, and hydrogen (180 sccm) and argon (350 sccm) as carrier gases. The water vapor concentration in the CVD chamber was controlled at 775 ppm by bubbling a small amount of argon gas through water.

The nanotube fibers were produced from the MWNT forests by using tweezers to contact the sidewall and then hand-drawn at a speed of ~50 cm/min. The as-drawn fibers were physically twisted using a motorized drive at 500 rpm. The twisted fibers were passed through ethanol to provide permanent twisting. The cross-sections of the fibers were obtained using the microtoming technique. The fibers for cross-sectioning were immersed in the mixture of methyl methacrylate (75 mL), dibutyl phthalate (5 mL), and benzoyl peroxide (2.5 g). The mixture was then polymerized at 37 °C under vacuum overnight. The fibers embedded in the polymer resin were then cut into slices by a diamond knife. The specimens were coated with a fine gold layer by ion-sputter.

Morphology and microstructure of the fibers and their cross-sections were studied using LEO 1530 scanning electron microscopy (SEM) at 5 kV and Hitachi HF-2000 transmission electron microscopy (TEM) at 200 kV. Cross-sectional areas were determined using Image Tool software. This software is part of Microsoft Windows 9x.

Raman spectra were collected in the back scattering geometry using Holoprobe Research Raman Microscope made by Kaiser Optical System using 785-nm excitation laser with polarizer. X-ray diffraction patterns were obtained on multi-filament bundles on Rigaku Micromax-002 ($\lambda = 0.15418$ nm) using Rigaku R-axis IV++ detection system. X-ray photoelectron spectroscopy (XPS) analysis was conducted on a model SSX-100 spectrometer (Surface Science Instruments). The tensile properties of the fibers were determined using RSA III solids analyzer (Rheometric Scientific, Co.) at room temperature at a gauge length of 25 mm and a strain rate of 0.2 mm/min. The single fibers were carefully glued with epoxy onto the heavy paper tabs, which were then mounted on to RSA grips. Once in the tensile tester, the paper tabs were cut down by scissors, leaving the fibers without damage. For each fiber, at least five samples were tested.

Results and discussion

Figure 1 shows SEM images of 1-mm high MWNT forest grown at 750 °C for 20 min. The MWNTs are five to seven walls and ~10 nm in outer diameter. The nanotubes contain very little amorphous carbon based on the TEM images (inset in Fig. 1a). A close examination of the forest under SEM reveals that the nanotubes are vertically aligned along the growth direction and appear to be entangled

Fig. 1 SEM images of an MWNT forest for fiber spinning: (a) 1-mm high vertically standing MWNT forest grown by water-assisted CVD growth. Inset, high resolution TEM image of an individual nanotube. (b) Forest wall. The circle shows aligned CNTs with entangled branches. (c, d) Top and bottom of the forest. The circles reveal entangled network

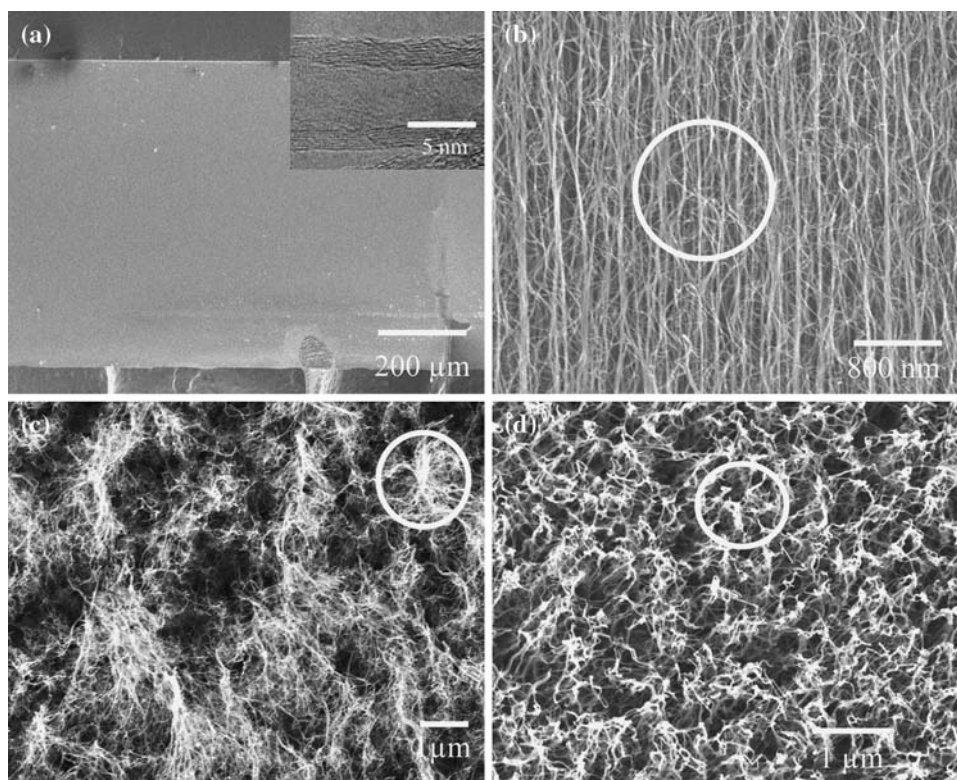


(Fig. 1b–d). XPS survey scans on the top and bottom of MWNT forests show only carbon (eV \sim 285 C1s) with the absence of iron catalysts (eV \sim 710 Fe2ps) (Fig. 2). These results demonstrate that the as-grown MWNT forests are of high purity. The fiber drawing is shown in Fig. 3. As-drawn fibers appeared as aerogel ribbons whose width and thickness were controlled by the forest sidewall width used for spinning fibers. The ribbon-like aerogel fibers spun from the 1-mm wide sidewall had width of \sim 80 μ m and thickness of \sim 15 μ m. About 1-m long CNT fibers were

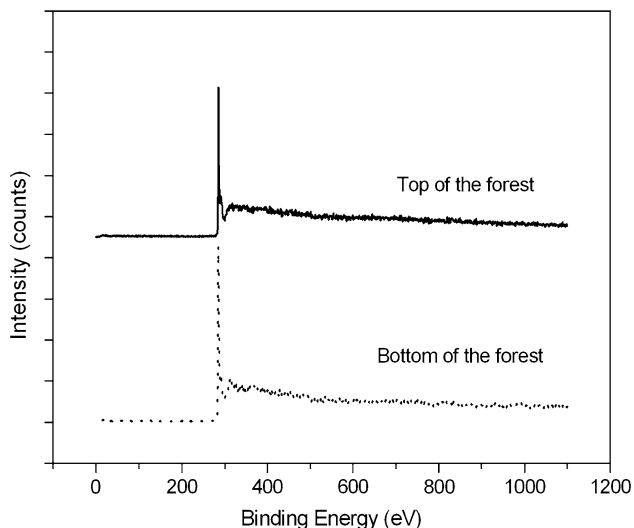


Fig. 2 XPS scans of top and bottom of the nanotube forest

spun out for easy handling by hand, although there was no theoretical limit on the drawn length for this dry-drawing processing.

Figure 4a, b shows SEM images of as-drawn nanotube fibers. The spacing between nanotubes in this aerogel fiber varies from tens to hundreds of nanometer (Fig. 4b). The as-drawn aerogel fibers easily stick to the surface of another object and therefore it is difficult to handle them for most practical applications. We densified the as-drawn aerogel fibers by passing them through ethanol [11, 15]. After ethanol evaporation, the aerogel fibers were densified

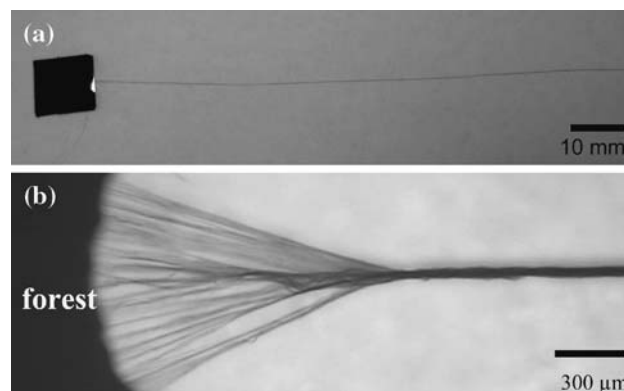
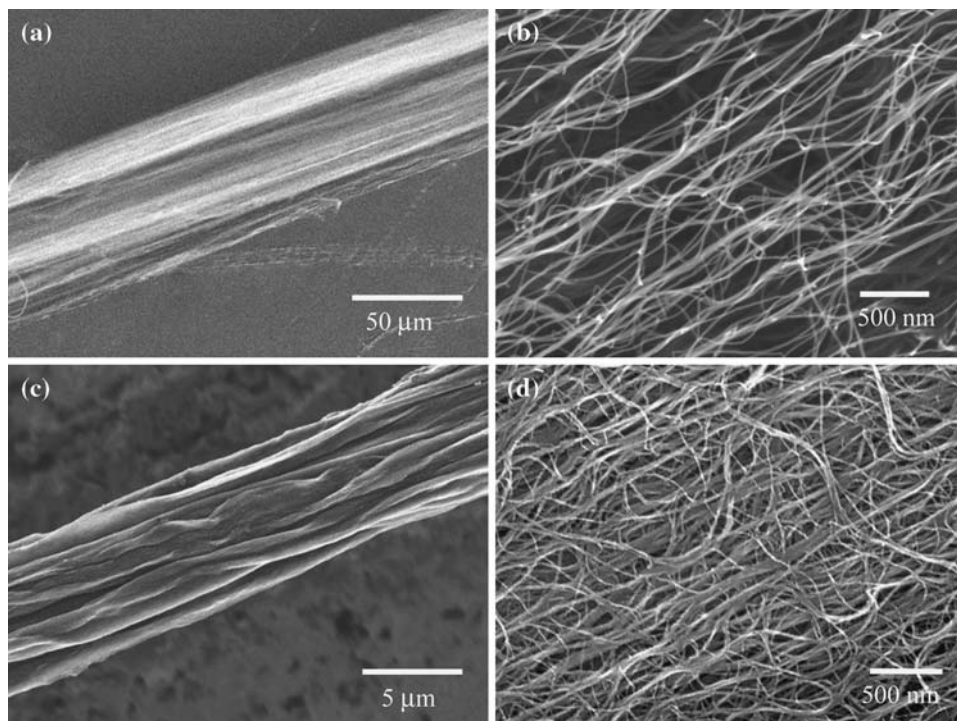


Fig. 3 Spinning continuous MWNT fibers from the forest: (a) Photograph of the fiber in the process of being drawn from the 10 mm \times 10 mm forest; (b) optical image showing the nanotubes being pulled from the forest wall into a fiber

Fig. 4 SEM images of neat MWNT fibers: (a) As-drawn aerogel fiber; (b) nanotube arrangements in the as-drawn fiber; (c) densified fiber, and (d) nanotube arrangement in the densified fiber



into compact fibers with transverse dimension of about $12 \mu\text{m} \times 5 \mu\text{m}$ (Fig. 4c, d).

Nanotube orientation in the fiber was studied using Raman microscopy. The Raman ratios $I_{G,0^\circ}/I_{G,90^\circ}$ were determined from the peak density of G-band at ca. $1,590 \text{ cm}^{-1}$ for polarization parallel and perpendicular to the fiber axis. The values for as-drawn aerogel fiber and densified fiber were calculated to be 2.7 and 2.2, respectively (Fig. 5), indicating a small decrease in nanotube orientation during densification.

The nanotube alignment in the densified fiber was also determined by wide-angle X-ray diffraction (WAXD). A two-dimensional (2D) WAXD pattern shows Bragg diffraction on the equator at $2\theta = 25.2^\circ$ (Fig. 6a), corresponding to the graphite (002) plane in the nanotubes with a d spacing of 0.353 nm. This value is 0.011 nm larger than the previously reported value of 0.341 nm of arc-discharge or laser ablation produced MWNTs [20], suggesting that the CVD-produced MWNTs in this work are somewhat more disordered. The crystal size deduced from (002) Bragg peak is ~ 2.0 nm, which is consistent with the TEM result of 5–7-walled MWNTs (inset of Fig. 1a). The azimuthal scan of the (002) Bragg diffraction was obtained (Fig. 6b) by plotting 2D data as intensity I versus azimuthal angle ϕ . The full width at half-maximum of the curve is 33.0° , indicating that the aligned nanotubes have a mosaic angle of $\pm 16.5^\circ$ around the fiber axis.

Twisting can enhance stress transfer between nanotubes under tensile forces [21, 22]. However, the twisted CNT fibers were not stable and tended to relax (untwist and coil) under unconstrained environments [23]. Twisted CNT fibers were passed through ethanol and effectively stabilized after complete ethanol evaporation (Fig. 7).

The fiber cross-sectional areas were measured from SEM images (Fig. 8), which were used to calculate the mechanical properties of the fibers. Figure 9 shows the typical stress–strain curves of densified fiber, twisted fiber,

Fig. 5 Raman G-band spectra for (a) as-drawn aerogel fiber and (b) densified fiber. The angle between polarizer and the fiber axis are 0 and 90°

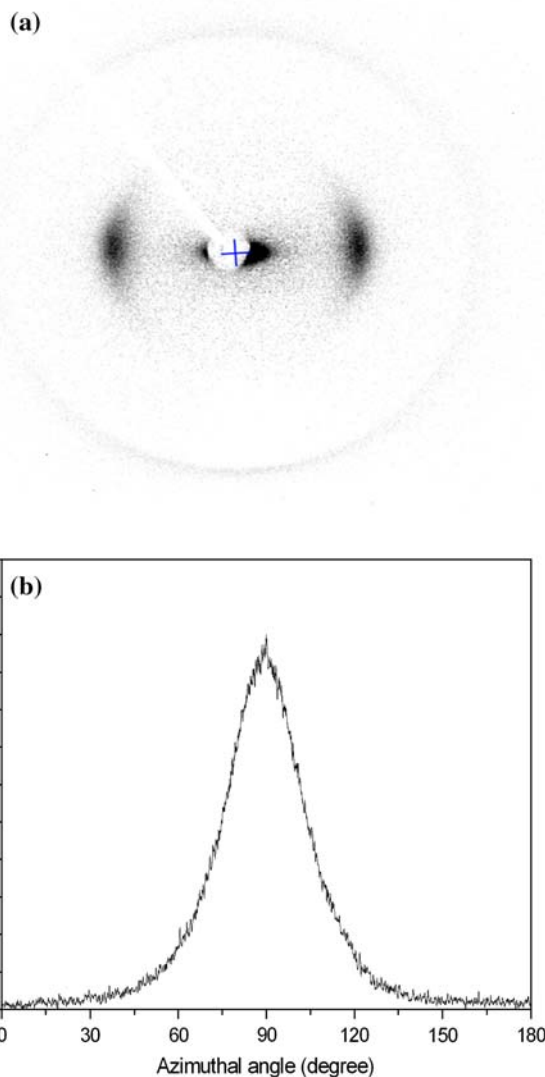
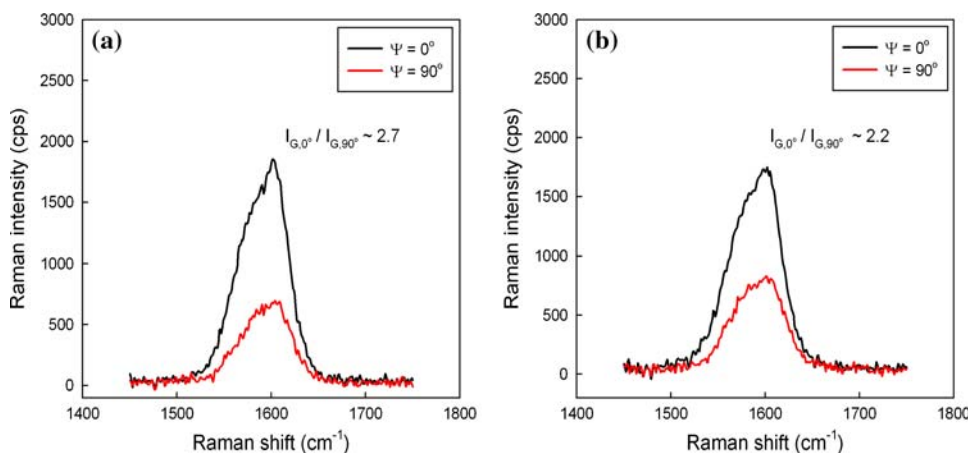


Fig. 6 (a) WAXD pattern of densified MWNT filaments. (b) The azimuthal intensity scan of the (002) reflection

Fig. 7 SEM images of twisted fibers with densification: (a) single fiber; (b) nanotube arrangement in the fiber; (c) nanotube fiber knot, and (d) double twisted fiber. Arrow shows the direction of the fiber axis

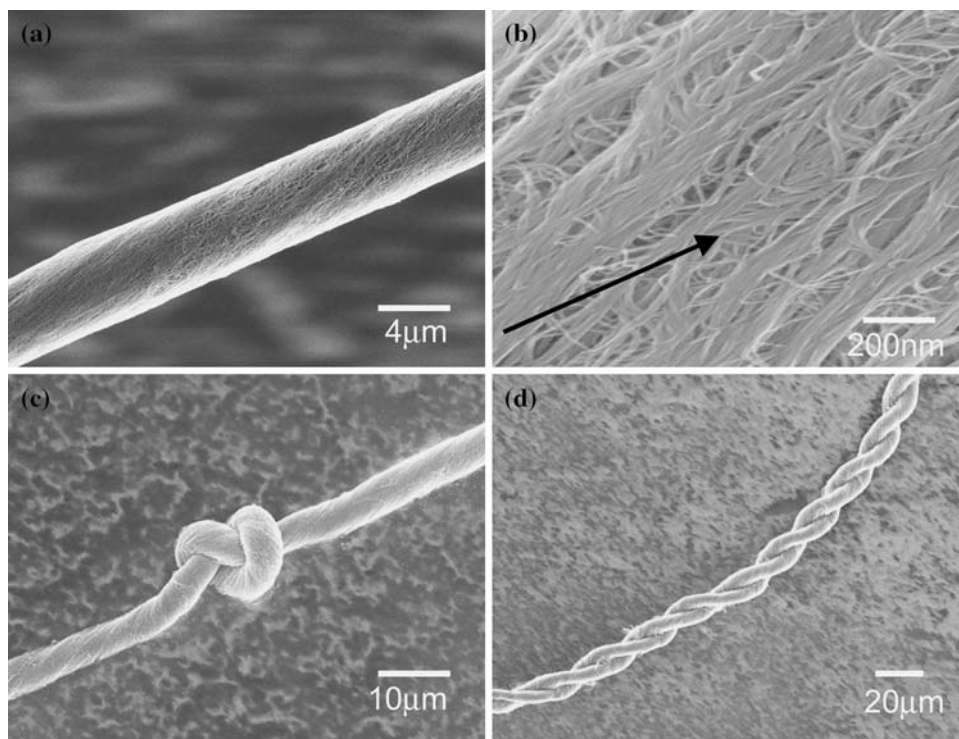
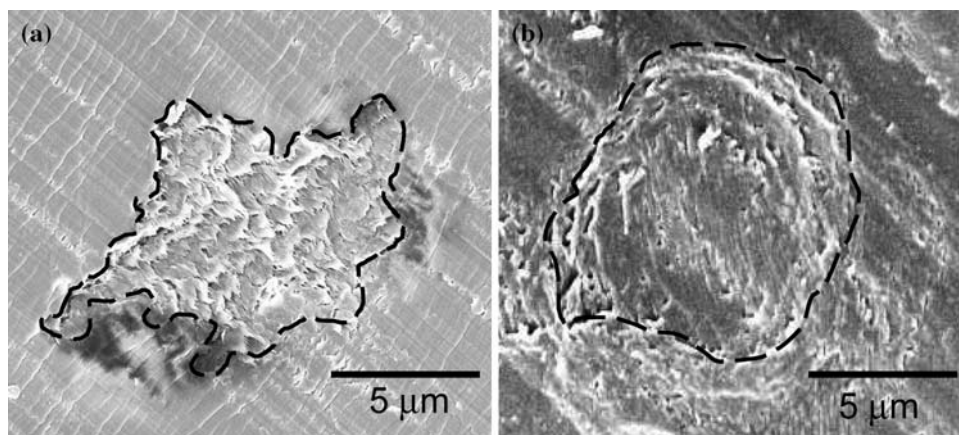


Fig. 8 SEM images of cross-sections: (a) densified fiber and (b) twisted fiber. Dash lines highlight the cross-sectional boundary



and twisted fiber with densification and the data are listed in Table 1. With twisting, tensile strength increased and Young's modulus decreased which are expected because of efficient load transfer and reduction of nanotube orientation [24]. Twisting increased the strain-to-failure, resulting in the enhanced energy needed to break the fiber (called toughness). The work of rupture of twisted and densified nanotube fibers is ~ 30 J/g, which is six times the toughness of the densified fiber (Table 1). It is interesting to note that the T&D nanotube fibers exhibit two linear regions, which correspond to two values of Young's modulus. The low modulus initial region is due to high twisting. After the initial region, the Young's modulus of the fibers increases $\sim 100\%$. It is assumed that this process corresponds to

re-orientation of the nanotubes in the fibers during the stretching and is analogous to the effect of those of the twisted yarn [25].

It should be noted that the tensile strength (0.50 ± 0.10 GPa) of the fiber from 1.0-mm long nanotubes in this work is higher than values of 0.3 and 0.4 GPa for the dry-drawn fibers (with similar ~ 10 - μm diameters) from 0.3 to 0.65-mm long nanotubes, respectively (Table 1) [12, 13]. Longer nanotubes will increase inter-tube contact areas and therefore yield higher tensile strength. Decreasing the fiber diameter may further increase the tensile strength, as observed in Ref. [13] (Table 1). It is reported that the tensile strength of the dry-drawn fibers from 0.65 mm long nanotubes with a ~ 3 - μm

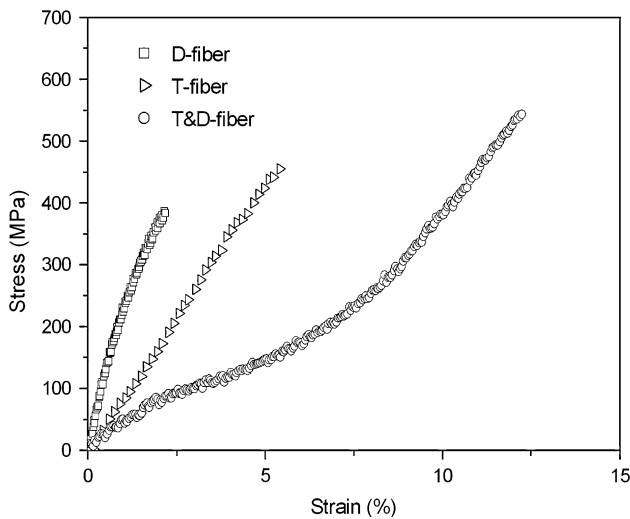


Fig. 9 Stress–strain curves of different MWNT fibers: densified fiber (D-fiber), twisted fiber (T-fiber), and twisted fiber with densification (T&D fibers)

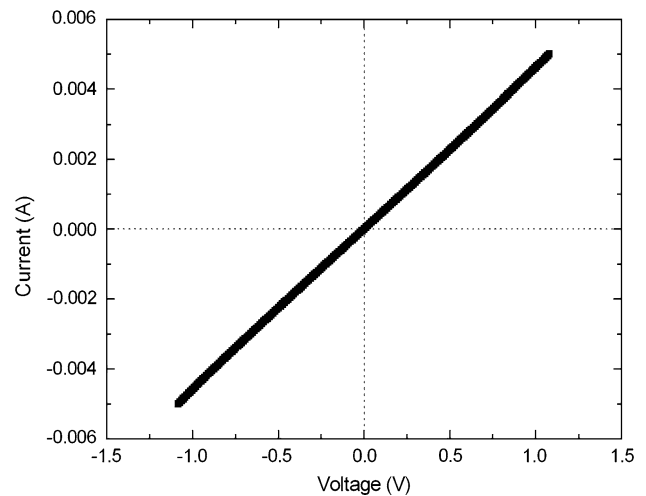


Fig. 10 Current (I)–voltage (V) plot of a densified MWNT fiber

Table 1 Data of mechanical properties for the post-treated dry-drawn CNT fibers

Samples	Strength (GPa)	Modulus (GPa)	Elongation (%)	Work of rupture (J/g)
D-fibers	0.35 ± 0.07	25 ± 5	2.2 ± 0.2	5 ± 1
T-fibers	0.40 ± 0.08	10 ± 2	5.0 ± 1.0	11 ± 2
T&D-fibers	0.50 ± 0.10	8.0 ± 1.0	11.0 ± 3.0	30 ± 4
Ref. [12] ^a	0.15–0.30	2–28	Up to 13%	~ 14
Ref. [13] ^b	0.17–0.41	89–241	1.8–2.4	–
	0.85–1.91	275–330	2.2–7.0	–
Ref. [25] ^c	0.44 (2.2 N/Tex)	32 (160 N/Tex)	4–8	30–60

^a The dry-drawn fibers were produced from 0.3-mm long nanotubes

^b The dry-drawn fibers were produced from 0.65-mm long nanotubes. The first row values are from 10 to 13- μ m diameter fibers while the second row values are from 3 to 4- μ m diameter fibers

^c The fibers were produced by CVD method and consisted of collapsed nanotubes

diameter could reach 1.91 GPa (Table 1) [13]. Our results are comparable to the average value of 0.44 GPa from CVD aerogel drawn fibers recently reported by Windle and co-workers (Table 1) [25].

The DC electrical conductivity of the densified nanotube fibers was measured along the fiber axis using a two-point probe. The current–voltage (I–V) curve of the MWNT fiber is linear (Fig. 10). The fibers from 1-mm long nanotubes had room temperature axial conductivity of $\sim 5.0 \times 10^4$ S/m. This result can be favorably compared to the previous reported values of 3.0×10^4 and 4.0×10^4 S/m for the dry-drawn MWNT fibers from 0.3 mm nanotubes and from 0.65 mm nanotubes, respectively [12, 13]. The somewhat higher electrical conductivity of the MWNT fiber in this work may be attributed to longer nanotubes with fewer junctions [26, 27].

Conclusions

In summary, we have reported that millimeter-long water-assisted CVD grown CNTs can be directly dry-drawn into continuous nanotube fibers. As-drawn CNT fibers are aerogel and can be transformed into more compact fibers by twisting or passing through a volatile liquid such as ethanol. We observe that the ethanol can also stabilize twists in the fiber. The toughness of the twisted and densified fibers is six times the toughness of densified fibers.

Acknowledgements Financial support from the Air Force Office of Scientific Research (FA9550-06-1-0315) and from the National Aeronautics and Space Administration (UCF-FY-04) are gratefully appreciated.

References

1. Vigolo B, Penicaud A, Coulon C, Sauder C, Railer R, Journet C, Bernier P, Poulin P (2000) *Science* 290:1331
2. Dalton AB, Collins S, Munoz E, Razal J, Ebron VH, Ferraris JP, Coleman JN, Kim BG, Baughman RH (2003) *Nature* 423:703
3. Miaudet P, Badaire S, Maugey M, Derre A, Pichot V, Launois P, Poulin P, Zakri C (2005) *Nano Lett* 5:2212
4. Zhu HW, Xu CL, Wu DH, Wei BQ, Vajtai R, Ajayan PM (2002) *Science* 296:884
5. Li YL, Kinloch IA, Windle AH (2004) *Science* 304:276
6. Motta M, Li YL, Kinloch I, Windle A (2005) *Nano Lett* 5:1529
7. Ericson LM, Fan H, Peng H, Davis VA, Zhou W, Sulpizio J, Wang Y, Booker R, Vavro J, Guthy C, Para-Vasquez ANG, Kim MJ, Ramesh S, Saini RK, Kittrell C, Lavin G, Schmidt H, Adams WW, Billups WE, Pasquali M, Hwang WF, Hauge RH, Fischer JE, Smalley RE (2004) *Science* 305:1447
8. Davis VA, Ericson LM, Parra-Vasquez ANG, Fan H, Wang Y, Prieto V, Longoria JA, Ramesh S, Saini RK, Kittrell C, Billups WE, Adams WW, Hauge RH, Smalley RE, Pasquali M (2004) *Macromolecules* 37:154
9. Wang YH, Ericson LM, Kittrell C, Kim MJ, Shan HW, Fan H, Ripley S, Ramesh S, Hauge RH, Adam WW, Pasquali M, Smalley RE (2005) *Chem Mater* 17:6361
10. Jiang KL, Li QQ, Fan SS (2002) *Nature* 419:801
11. Zhang XB, Jiang KL, Feng C, Liu P, Zhang L, Kong J, Zhang TH, Li QQ, Fan SS (2006) *Adv Mater* 18:1505
12. Zhang M, Atkinson KR, Baughman RH (2004) *Science* 306:1358
13. Zhang XF, Li QW, Tu Y, Li Y, Coulter Y, Zheng L, Zhao Y, Jia Q, Peterson DE, Zhu YT (2007) *Small* 3:244
14. Hata K, Futaba DN, Mizuno K, Namai T, Ymura M, Iijima S (2004) *Science* 306:1362
15. Futaba DN, Hata K, Yamada T, Hiraoka T, Hayamizu Y, Kakudate Y, Tanaike O, Hatori H, Yumura M, Iijima S (2006) *Nat Mater* 5:987
16. Zhu LB, Xiu YH, Hess DW, Wong CP (2005) *Nano Lett* 5:2641
17. Zhu LB, Sun YY, Hess DW, Wong CP (2006) *Nano Lett* 6:243
18. Yamada T, Namai T, Hata K, Futaba DN, Mizuno K, Fan J, Yudasaka M, Yumura M, Iijima S (2006) *Nat Nanotech* 1:131
19. Baughman RH (2006) *Nat Nanotech* 1:94
20. Lin L, Bower C, Zhou O (1998) *Appl Phys Lett* 73:1197
21. Qian D, Liu WK, Ruoff RS (2003) *Compos Sci Technol* 63:1561
22. Pipes RB, Hubert P (2002) *Compos Sci Technol* 62:419
23. Bradford P, Fang S, Zhang M, Baughman RH (2007) *SAMPE J* 43:2
24. Hearle JWS, Grosberg P, Backer S (1969) *Structural mechanics of fibers, yarns and fabrics*. Wiley, New York
25. Motta M, Moisala A, Kinloch IA, Windle AH (2007) *Adv Mater* 19:3721
26. Hecht D, Hu L, Gruner G (2006) *Appl Phys Lett* 89:133112
27. Balberg I, Binenbaum N, Anderson CH (1983) *Phys Rev Lett* 51:16056